# Research on Positioning Accuracy of Indoor and Outdoor Pedestrian Seamless Navigation

Kailong Wang, Huixia Li(✉), and Hang Guo

Nanchang University, Nanchang 330031, China
lihuixia0601@163.com

**Abstract.** The accuracy of pedestrian positioning is helpful to ensure the pedestrian safety in both indoor and outdoor environments. Improve the accuracy of pedestrian positioning is a key research issue. In order to solve the problem that the indoor and outdoor pedestrian navigation is not continuous and the accuracy is low, a pedestrian seamless navigation and positioning method based on BDS/GPS/IMU is proposed. In outdoor environment, in order to improve the availability of dynamic positioning when the single-system observation geometry is not ideal, the key techniques such as the differential coordinates and time benchmark in BDS/GPS positioning are studied, and a method of eliminating time difference by the independent combination difference in the system is proposed. This method simplifies the operation steps and overcomes the current compatible positioning difficulties without the time difference between BDS and GPS. It can be seen that the more the number of visible satellites, the better the space geometric distribution. In the combined positioning experiment results of BDS and GPS, the number of visual satellites are about 6–8 when GPS is used alone. When using the combined system, the number of visible satellites increased to about 16. The increase in the number of visible satellites greatly improves the observation geometry. For the Position Dilution of Precision (PDOP), the maximum PDOP of the dual system is 2.7, which is significantly lower than that of the single system, and the observation geometry performance is greatly improved. In the effective positioning time, for BDS/GPS, the positioning accuracy of elevation (U) direction is better than 4 cm, and the positioning accuracy of North (N) and East (E) direction is better than 2 cm. Based on the analysis of pedestrian gait characteristics, a multi-condition constrained zero-velocity detection algorithm is proposed. For the error of the inertial sensor error is accumulated over the time, the zero velocity update (ZUPT) algorithm is implemented to correct the cumulative errors by using to the designed extended Kalman filter (EKF) with the velocity and angular velocity information as the measurements. The results show that the accuracy of dual-mode positioning system of BDS compatible with GPS is better than the single-mode GPS positioning, the outdoor position accuracy can reach centimeter level, and under ZUPT compensation the indoor error ratio is 1%, which can achieve more accurate pedestrian seamless navigation.

**Keywords:** Pedestrian seamless navigation · BDS/GPS · Zero Velocity Update (ZUPT) · Extended Kalman Filter (EKF)


Y.-D. Zhang et al. (Eds.): ICMTEL 2020, LNICST 327, pp. 355–367, 2020.
https://doi.org/10.1007/978-3-030-51103-6_32

## 1 Introduction

In a closed environment without satellite signals, the pedestrian navigation system can achieve independent positioning. It can be effectively used in emergency rescue, jungle adventure and military fields, and in recent years it has become a research hotspot in the field of navigation.

At present, many scholars have studied the indoor and outdoor positioning technology. The positioning technology in document [1–10] requires pre-installation of the sensor network, using time difference of arrival (TDOA), angle of arrival (AOA), signal strength and other algorithms to achieve indoor positioning, but the navigation range is limited. The document [11] proposed an indoor navigation system based on GPS/IMU/Zigbee, using Zigbee to establish a fingerprint database fusion with IMU, and combined with GPS to achieve positioning, but single GPS signal is easy occluded, it needs to establish complex Zigbee nodes fingerprint database in advance, and the IMU solution error diverges over time, the positioning accuracy is not high. Document [9–12] studied the pseudolite-based positioning technology, and used the pseudolite to launch the satellite-like signals to achieve indoor navigation, however, this method is influenced by multipath effect, it is not suitable for indoor complex environment. In document [13], a monocular vision indoor positioning technology is studied. It collects images, extracts feature points, and gets position through the coordinate transformation, but the computation is large, and the image extraction algorithm is complex, which requires the computer with fast speed and high power consumption.

Compared with the above algorithms, a navigation and positioning method based on the BDS/GPS/IMU is studied. The dual-mode positioning of BDS and GPS not only extends the advantages of single-satellite, but also achieves the common coverage of the dual-mode navigation system at the same time and the same place, relieves the influence of factors such as terrain, obstacles, and so on. In indoor positioning, uses the MEMS-IMU equipment with small size, low cost and autonomous navigation module, improves the pedestrian dead reckoning algorithm (PDR). At same time, by increasing the constraint conditions, the pedestrian zero speed state is accurately determined, and adopts ZUPT and zero angular velocity update (ZARU) to auxiliary correct the angular velocity update further eliminates the cumulative error of the inertial device. The system has strong autonomous positioning and better navigation continuity even in complex environments. This method can achieve high-accuracy indoor and outdoor pedestrian navigation.

## 2 The Positioning Method of BDS/GPS

Because of the difference between the BDS and the GPS in the definition of coordinate and the time system, in order to realize the dual-mode positioning, it is necessary to solve the transformation and unification of the space-time coordinate. Ignoring the coordinate changes in the two system coordinate system, it only needs to solve the deviation problem between different systems [14–16]. In order to simplify the calculation, the time deviation can be eliminated by the form of the difference algorithm between the systems. In the process of observation, the base station receiver and the

rover station receiver simultaneously observed multiple BDS satellites and GPS satellites. Among them, two BDS satellite and two GPS satellites were selected to further operation, obtained the respective carrier phase observation equations between the satellites, and then calculated the difference equation between the satellites and the receivers. Therefore, we can get two equations about the respective satellites, the simultaneous equation is the combined positioning double difference observation equations [17].

$$\begin{bmatrix} \nabla\Delta\Phi_{AB}^{G} \\ \nabla\Delta\Phi_{AB}^{C} \end{bmatrix} = \begin{bmatrix} \nabla\Delta\rho_{AB}^{G} - \lambda^{G}\nabla\Delta N_{AB}^{G} + \nabla\Delta Trp_{AB}^{G} + \varepsilon_{\nabla\Delta}^{G} \\ \nabla\Delta\rho_{AB}^{C} - \lambda^{C}\nabla\Delta N_{AB}^{C} + \nabla\Delta Trp_{AB}^{C} + \varepsilon_{\nabla\Delta}^{C} \end{bmatrix} \tag{1}$$

Which $\nabla\Delta\Phi_{AB}^{G}$, $\nabla\Delta\Phi_{AB}^{C}$ represent GPS and BDS carrier phase double-difference observations, $\nabla\Delta\rho_{AB}^{G}$, $\nabla\Delta\rho_{AB}^{C}$ represent GPS and BDS pseudo-range double-difference observations, $\lambda$ is the carrier wavelength, $\nabla\Delta N$ is the double-difference full-circumference ambiguity vector, and $Trp$ z is the tropospheric delay error, $\varepsilon_{\nabla\Delta}$ is the observation noise, and subscripts $A$ and $B$ represent the base station and the rover station, respectively.

The double-difference observation equation composed of BDS and GPS, not only eliminates most of the error such as the time deviation, but also as the distance between the two stations is relatively close, the error caused by multipath is small and can be ignored. According to Eq. (1), using the least squares method or Kalman filter to solve the double-difference full-circumference ambiguity $\nabla\Delta N$, and then the position coordinates can be solved.

## 3 Indoor Pedestrian Positioning Method

### 3.1 PDR Algorithm

The purpose of the pedestrian positioning system is to achieve positioning by using the MTI IMU device strapping onto a foot/shoe. The proposed PDR positioning method is implemented under the framework of the Extended Kalman Filter (EKF). The main idea of this project is to use these filtering algorithms to estimate the cumulative errors (biases) of the IMU sensors. When the foot is on the floor, the EKF is updated by the velocity and angular velocity measurements respectively by the Zero-Velocity-Update (ZUPT) and Zero-Angular-Rate-Update (ZARU). Then the sensor biases are compensated with the estimated errors. Therefore, frequent use of the ZUPT/ZARU measurements can assist in correcting the errors, so even relatively low cost sensors can provide useful navigation performance. The PDR system prepared in the Matlab environment consists of five algorithms:

1) Initial alignment, using the static data of the accelerometer and magnetometer for the first few minutes to calculate the initial attitude.
2) IMU mechanization algorithm for computing the navigation parameters (position, velocity and attitude).

3) Zero velocity detection algorithm for determining when the foot is on the ground, the velocity and angular velocity of the IMU are zero.
4) ZUPT and ZARU feed the EKF with the measured errors when pacing is detected.
5) EFK estimates the errors and gives feedback to the IMU mechanization algorithm.

### 3.2 Initial Alignment

The initial static alignment provides the initial attitude information for the navigation system. The initial alignment of the IMU sensor is accomplished by two steps: leveling and gyro compassing. Leveling refers to obtain the roll and pitch by using the acceleration, and gyro compassing refers to obtain the heading by using the angular velocity. However, the bias and noise of gyroscopes are larger than the value of the Earth's rotation rate for the micro-electronic mechanical system (MEMS) IMU, so the heading error is large. In this paper, the initial alignment of the MEMS IMU is completed by using the static data of accelerometer and magnetometer during the first few minutes, and a method of heading measurement using a magnetometer is proposed.

### 3.3 Zero Velocity Detection Process

The movement of the foot-mounted IMU can be divided into two phases. The first one is the swing phase that means the foot-mounted IMU is moving. The second one is the stance phase which means the foot-mounted IMU is on the ground. The angular velocity and linear velocity of the foot-mounted IMU must be very close to zero in the stance phase. Therefore, the angular velocity and linear velocity of the foot-mounted IMU can be zero as the measurements of the Extended Kalman Filter (EKF) [18–20]. This is the main idea of the ZUPT and ZARU method.

1) Acceleration amplitude detection. In the zero speed phase, the acceleration vector value of the pedestrian's foot changes around the gravitational acceleration. Therefore, the logical value of the moment is obtained by judging the relationship between the acceleration amplitude and the set threshold.

$$\left|\boldsymbol{a}_k^b\right| = \sqrt{{a_{x(k)}^b}^2 + {a_{y(k)}^b}^2 + {a_{z(k)}^b}^2} \tag{2}$$

$$c_1 = \begin{cases} 1, & T_{\min} < |a_k| < T_{\max} \\ 0, & others \end{cases} \tag{3}$$

2) Acceleration amplitude variance detection. Variance is an important condition for measuring the degree of dispersion of variables and averages. By setting the sliding window $w$, the variance of the data is obtained to determine the dispersion of the zero-speed point.

$$\sigma_{a_k}^2 = \frac{1}{2w+1}\sum_{j=k-w}^{k+w}(a_j - \bar{a}_k)^2 \tag{4}$$

$$c_2 = \begin{cases} 1, & \left|\sigma_{a_k}^2\right| < T_{\sigma\max} \\ 0, & others \end{cases} \tag{5}$$

3) Angular velocity amplitude detection. When in the zero speed interval, the angular velocity of the foot changes to be close to 0, and the logical value is obtained by judging the magnitude relationship between the modulus value of the angular velocity at time $k$ and the threshold value.

$$|\omega| = \sqrt{\omega_x^2 + \omega_y^2 + \omega_z^2} \tag{6}$$

$$c_3 = \begin{cases} 1, & |\omega_k| < T_{\omega\max} \\ 0, & others \end{cases} \tag{7}$$

4) Peak acceleration detection. To determine the acceleration peak of $\Delta t$ t between the two times before and after the vertical direction, $\Delta t$ t is the zero speed interval.

$$a_{\max}(k) = \begin{cases} a_z(k) < T_{\max} \\ a_z(k) < a_z(k-1) \\ a_z(k) < a_z(k+1) \end{cases} \tag{8}$$

$$C_4(k+\Delta t_1, k+\Delta t_2) = \begin{cases} 1, & a_{\max}(k) \rightarrow true \\ 0, & others \end{cases} \tag{9}$$

According to the above four constraints, the conditional threshold is set respectively, and the obtained judgment result is calculated by the relationship of logical "AND", the equation is as follows:

$$C = C_1 \,\&\, C_2 \,\&\, C_3 \,\&\, C_4 \tag{10}$$

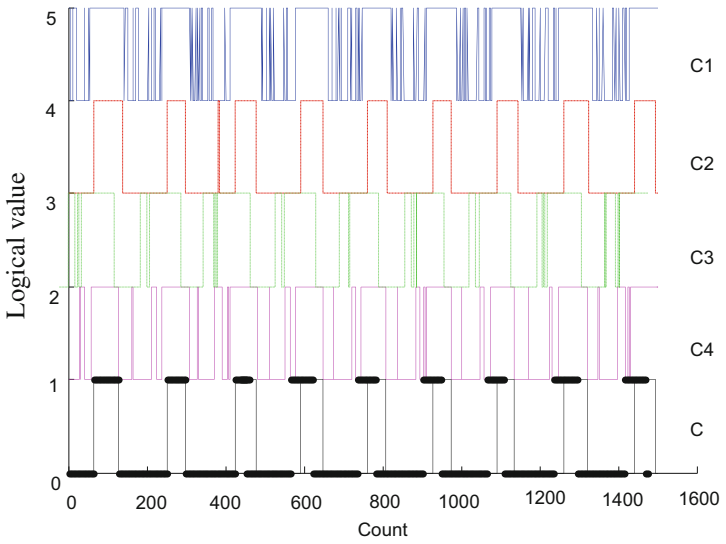


**Fig. 1.** The logical value of zero velocity detection

When $C$ is 1, the zero speed interval. Figure 1 shows the pedestrian zero velocity detection experiment. The figure captures the data of 9 steps of pedestrian walking. It shows that the algorithm results are consistent with the actual number of steps, which indicates that the algorithm accurately determines the zero velocity phase of pedestrians.

## 4 Experiment and Analysis

The receiver equipment used in the experiment can receive GPS and BDS signals, and the IMU includes a three-axis gyroscopes, accelerometers, and magnetometers, technical specifications of these three sensors are show in Table 1. The sampling frequency of the receiver is 1 Hz, the cut-off angle is 10°, and the IMU sampling frequency is 100 Hz. In the experiment, we selected a path from outdoor to indoor, as shown in Fig. 2, it is the experimental environment for aerial photography. Fixed the base station antenna on the rooftop, fixed IMU on the pedestrian's foot, and handheld rover station receiver at the same time, after initial alignment, follow the route and walk normally to collect data.

**Table 1.** Sensor specification

| Technical specification | Gyroscopes | Accelerometers | Magnetometers |
|---|---|---|---|
| Standard full range | ±300 deg/s | ±50 $m/s^2$ | ±700 mGauss |
| Zero stability | 5 deg/s | 0.02 $m/s^2$ | 0.5 mGauss |
| Noise density | 0.1 deg/s/$\sqrt{Hz}$ | 0.02 $m/s^2$ $\sqrt{Hz}$ | 0.5 mGauss |

When the pedestrian is outside, the satellite signal is good and the BDS/GPS positioning is effective. In order to verify the superiority of BDS/GPS dual-mode positioning to the single-satellite system, the BDS/GPS fusion data and GPS data were calculated by GrafNav software respectively, and the Kinpos software developed by Wuhan University was used to process the data of the single BDS system. The standard deviations of the East, north, and up components of the three solutions are given in Figs. 3, 4 and 5. Table 2 summarizes the root mean square error of each component of the three schemes.

**Table 2.** RMS of GPS/BDS

| Constellation | E/m | N/m | U/m |
|---|---|---|---|
| GPS | 0.011 | 0.012 | 0.022 |
| BDS | 0.007 | 0.018 | 0.024 |
| BDS/GPS | 0.008 | 0.0067 | 0.018 |

Through three kinds of solving methods, the observation data is dynamically located by each epoch, and the epochs participating in the solution are all fixed. The positioning accuracy of each component is less than 3 cm, the average error of the horizontal position of the BDS/GPS system is less than 1.1 cm, and the accuracy is improved by 5 mm to 8 mm. During the experiment, the walking route gradually approaches the indoor environment from the outdoor. Due to the obstruction of obstacles such as walls, the error fluctuates when walker is entering into the indoor environment. The maximum horizontal error of GPS and BDS single system is 0.04 m and 0.03 m, respectively, while the maximum horizontal error of combined system is 0.028 m. It indicates that under the influence of obstacles and other factors, the BDS/GPS dual-system can reduce the error and improve the positioning accuracy compared with the single system (Table 2).

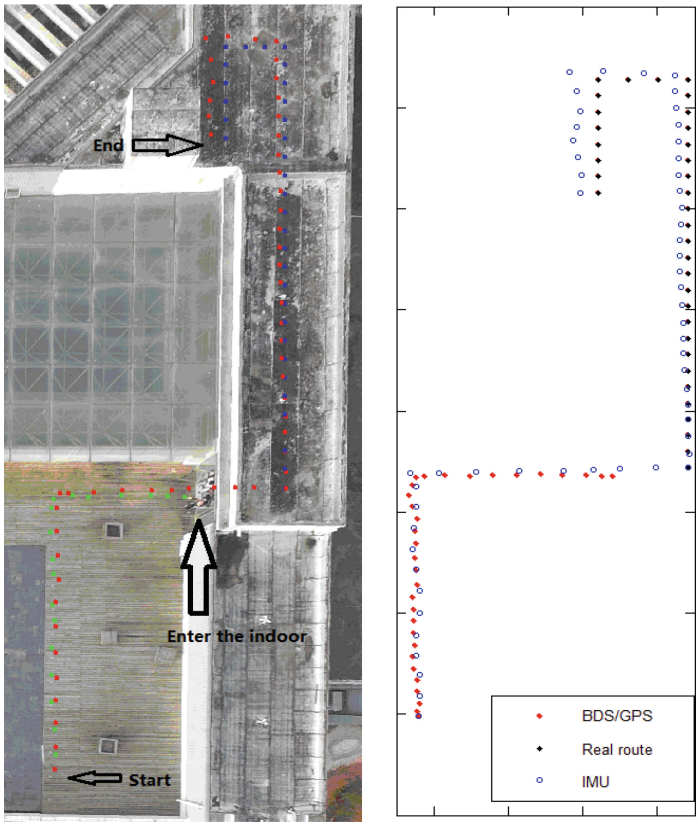


**Fig. 2.** Experimental environment and data processing

The average error of the BDS and GPS combination solution is 1.08 cm, and the positioning accuracy can reach the centimeter level. The main reason for the improved positioning accuracy of the combined dual-mode BDS and GPS positioning system is that the joint solution increases the number of spatial visible satellites, improves the geometric distribution of satellite and reduces the value of PDOP that affects the positioning accuracy. As shown in Table 3, the PDOP value is reduced due to the increase of the number of satellites. The smaller the PDOP, the better the accuracy of the positioning, therefore, the BDS/GPS dual-mode positioning accuracy is higher than that of the single system.

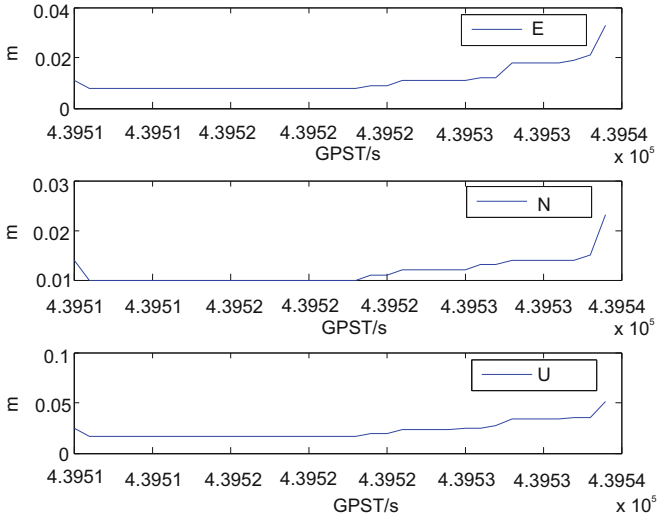


**Fig. 3.** GPS position error estimation

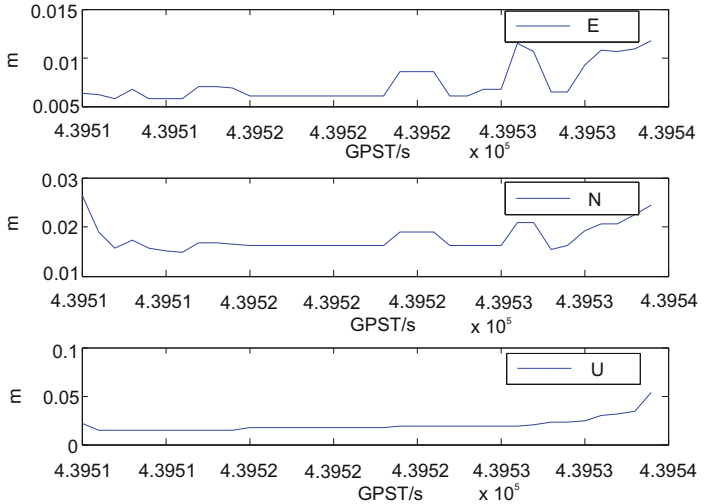


**Fig. 4.** BDS position error estimation

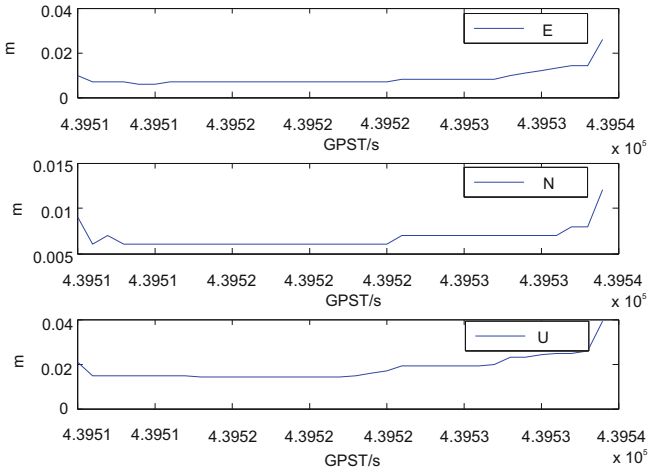


**Fig. 5.** GPS/BDS position error estimation

**Table 3.** Visual satellite number and PDOP value of each system

| Constellation | Visual satellite number | | | PDOP | | |
|---|---|---|---|---|---|---|
| | MAX | MIN | AVG | MAX | MIN | AVG |
| GPS | 9 | 5 | 8.3 | 3.3 | 1.3 | 1.73 |
| BDS | 9 | 5 | 7.7 | 3.64 | 2.11 | 2.41 |
| BDS/GPS | 18 | 10 | 16 | 2.7 | 1.1 | 1.4 |

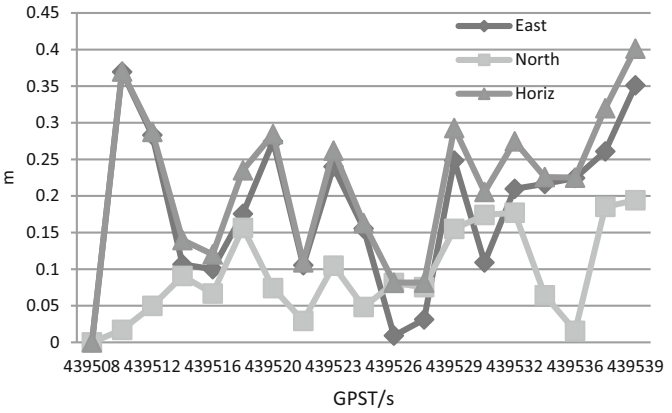


**Fig. 6.** IMU positioning error in the outdoor

At the same time, the outdoor IMU data is processed separately and compared with the satellite combination positioning. As shown in Fig. 7, the maximum absolute position error of the PDR algorithm is less than 0.4 m, which indicates that the algorithm achieves good results.

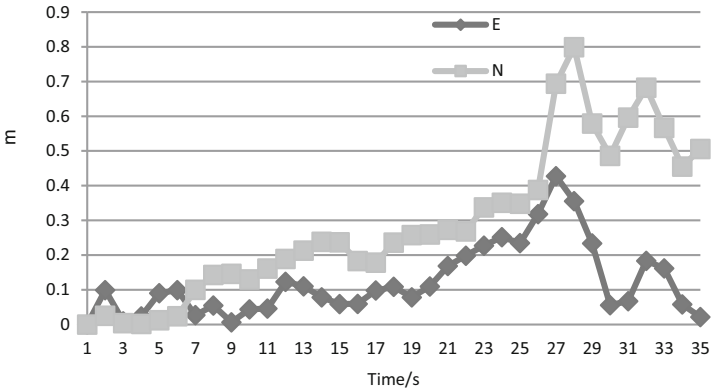


**Fig. 7.** PDR indoor positioning error

When the pedestrian entered the room, the BDS and GPS signal were interrupted, PDR algorithm was used to fix position. Table 4 shows the result of indoor navigation. The indoor algorithm results show that the average position errors in the East and the North are 0.102 m and 0.285 m respectively. The standard deviation in the East and the North are 0.123 m and 0.220 m, respectively. It can be seen that the zero velocity detection algorithm under multiple constraint conditions can improve the accuracy of step detection. Therefore, the zero velocity correction algorithm based on the EKF can significantly reduce the positioning divergence with time and reduce the positioning error, and realize seamless navigation between indoor and outdoor environments.

**Table 4.** Indoor positioning error

| | East/m | North/m |
|---|---|---|
| MIN | 0 | 0 |
| MAX | 0.427 | 0.799 |
| AVG | 0.102 | 0.285 |
| STD | 0.123 | 0.220 |

## 5 Conclusion

A higher precision method for seamless pedestrian navigation is proposed in this paper. Combined with the dual-mode positioning of BDS and GPS, the number of visible satellites can still be achieved in the relatively poor outdoor shelter, which makes the

geometric distribution of the observation satellites good, reduces the influence of multipath effect and other factors, and improves the positioning accuracy. In the environment where satellite signals cannot be received or mismatches, proposed the zero velocity multi-constraint conditions detection algorithm based on the Extended Kalman Filter (EKF), applied and updated with velocity and angular rate measurements by Zero-Velocity-Update (ZUPT) and Zero-Angular-Rate-Update (ZARU) solutions, greatly suppresses the influence of position divergence over time, and ensures the positioning accuracy when the satellite loses lock. The experimental results show that the outdoor position accuracy can reach centimeter level, and the indoor error ratio is about 1%, which realizes a high accuracy pedestrian seamless navigation method.

**Acknowledgments.** The paper was supported by the projects of the National Key R&D Program of China (Nos. 2016YFB0502204, 2016YFB0502002), National Natural Science Foundation of China (No. 41764002).

## References

1. Deng, Z., Yu, Y., Yuan, X., Wan, N., Yang, L.: Situation and development tendency of indoor positioning. China Commun. **10**(3), 42–55 (2013)
2. Popleteev, A.: Indoor Positioning using FM Radio Signals. University of Trento, Trento (2011)
3. Xu, Y., Ahn, C.K., Shmaliy, Y.S., et al.: Adaptive robust INS/UWB-integrated human tracking using UFIR filter bank. Measurement **123**, 1–7 (2018)
4. Xu, Y., Shmaliy, Y.S., Li, Y., Chen, X.: UWB-based indoor human localization with time-delayed data using EFIR filtering. IEEE Access **5**(1), 16676–16683 (2017)
5. Li, H.X., Wen, X., Guo, H., et al.: Research into kinect/inertial measurement units based on indoor robots. Sensors **18**(3), 839 (2018)
6. Xu, Y., Karimi, H.R., Li, Y.Y., Zhou, F.Y., Bu, L.L.: Real-time accurate pedestrian tracking using EFIR filter bank for tightly coupling recent inertial navigation system and ultra-wideband measurements. Proc. Inst. Mech. Eng. Part I-J. Syst. Control Eng. **232**(4), 464–472 (2018)
7. Guo, H., Li, H., Xiong, J., Yu, M.: Indoor positioning system based on particle swarm optimization algorithm. Measurement **134**, 908–913 (2019)
8. Xu, Y., Shmaliy, Y.S., Li, Y., Chen, X., Guo, H.: Indoor ins/lidar-based robot localization with improved robustness using cascaded fir filter. IEEE Access **7**(1), 34189–34197 (2019)
9. Xu, Y., Tian, G., Chen, X.: Enhancing INS/UWB integrated position estimation using federated EFIR filtering. IEEE Access **6**, 64461–64469 (2018)
10. Xu, Y., Chen, X.: Online cubature Kalman filter Rauch–Tung–Striebel smoothing for indoor inertial navigation system/ultrawideband integrated pedestrian navigation. Proc. Inst. Mech. Eng. Part I-J. Syst. Control Eng. **232**(4), 390–398 (2018)
11. Pany, T., Winkel, J., Riedl, B., Niedermeier, H., Eissfeller, B., Wörz, T., et al.: Experimental results from an ultra-tightly coupled GPS/Galileo/WiFi/ZigBee/MEMS-IMU indoor navigation test system featuring coherent integration times of several seconds. In: Satellite Navigation Technologies & European Workshop on GNSS Signals & Signal Processing, pp. 1–8. IEEE (2011)

12. Stone, J.M., Powell, J.D., Powell, P.J.D.: Precise positioning with GPS near obstructions by augmentation with pseudolites. In: IEEE Position Location and Navigation Symposium, pp. 562–569 (1998)
13. Sakamoto, Y., Niwa, H., Ebinuma, T., Fujii, K., Sugano, S.: Indoor positioning with pseudolites—the effect of the number of receivers and transmitters. In: Sice Conference, pp. 398–399 (2010)
14. Huang, J., Millman, D., Quigley, M., Stavens, D., Thrun, S., Aggarwal, A.: Efficient, generalized indoor WiFi GraphSLAM. In: 2011 IEEE International Conference on Robotics and Automation, pp. 1038–1043. IEEE (2011)
15. Junyong, C.: On the establishment of Chinese modern geodetic coordinate system. Board Geomat. Inf. Sci. Wuhan Univ. **27**(5), 441–44 (2002)
16. Li, J., Yang, Y., Xu, J., He, H., Guo, H.: GNSS multi-carrier fast partial ambiguity resolution strategy tested with real BDS/GPS dual- and triple-frequency observations. GPS Solut. **19** (1), 5–13 (2013)
17. Liang, W., Shen, L.Z., Hong, Y., Kai, Z.: Validation and analysis of the performance of dual-frequency single-epoch BDS/GPS/GLONASS relative positioning. Chin. Sci. Bull. **60** (9), 857 (2015). Opto-Electronics, A.O.
18. Caron, F., Duflos, E., Pomorski, D., Vanheeghe, P.: GPS/IMU data fusion using multisensor Kalman filtering: introduction of contextual aspects. Information Fusion **7**(2), 221–230 (2016)
19. Wendel, J., Meister, O., Schlaile, C., Trommer, G.F.: An integrated GPS/MEMS-IMU navigation system for an autonomous helicopter. Aerosp. Sci. Technol. **10**(6), 527–533 (2006)
20. Jiménez, A.R., Seco, F., Prieto, J.C., Guevara, J.: Indoor pedestrian navigation using an INS/EKF framework for yaw drift reduction and a foot-mounted IMU. In: 2010 7th Workshop on Positioning, Navigation and Communication, pp. 1–9. IEEE (2010)